

# Chaotic scattering on surfaces and collisional damping of collective modes

Klaus Morawetz, Michael Vogt, Uwe Fuhrmann  
*Fachbereich Physik, University Rostock, D-18055 Rostock, Germany*

Pavel Lipavský, Václav Špička  
*Institute of Physics, Academy of Sciences, Cukrovarnická 10, 16200 Praha 6, Czech Republic*

The damping of hot giant dipole resonances is investigated. The contribution of surface scattering is compared with the contribution from the interparticle collisions. A unified response function is presented which includes surface damping as well as collisional damping. The surface damping enters the response via the Lyapunov exponent and the collisional damping via the relaxation time. The former one is calculated for different shape deformations of quadrupole and octupole type. The surface as well as the collisional contribution each reproduce the experimental value, therefore we propose a proper weighting between both contributions related to their relative occurrence due to collision frequency between particles and of particles with the surface. Experimental data can be reproduced. We find that for low and high temperatures the collisional contribution dominates whereas the surface damping is dominant around temperatures of a third of the centroid energy.

## I. INTRODUCTION

The damping mechanisms of collective motions in excited nuclei are a topic of current debate. Mainly two lines of thought can be recognized. One believes that collisions are the physical reason for damping only - this is developed from the Fermi liquid understanding with bulk matter properties [1–14]. The other considers new features of the finite nucleus like surface oscillations and finite spacing of level density. Partially the investigations are performed without inertia [15–23] or including inertia [21,24–29] which is absent in infinite matter.

Both models predict a comparable quantity of damping necessary to reproduce the experimental data. Consequently, the question of correctness of one or the other physical reason for damping has been opposed. Of course, the correct description has to assume a finite nucleus consisting of nucleons which are bound via the mean field, through which the nucleons undergo mutual collisions and where the surface is formed by the particles itself. These features have been believed to be included in BUU simulations [30–32] or its nonlocal extensions [33]. In full simulations we will not get a simple insight into the physical origins of damping mechanism, how much are due to surface and how much are due to collisional contributions, however.

The aim of this article is to compare both pictures in the frame of linear response. Within the collision free Vlasov equation the linear response of finite systems is well known [34] and allows one to calculate the strength function of finite nuclei. The damping is, however, not reproduced since collisions are absent.

To include damping, we can take into account on the one hand the collisional damping in infinite matter and find a scaling for finite size effects in the sense of Thomas-

Fermi local density approximation. On the other hand we can consider the boundary of the finite nucleus as a fixed surface such that the nuclei perform a simple billiard bouncing off this wall. Provided we accept this simple picture it is possible to compare the damping caused by this chaotic scattering with the wall and the damping from collisional contributions. We will derive a response function which includes the additional chaotic process and find a total damping rate  $\Gamma = \Gamma_{\text{coll}} + \Gamma_{\text{surf}}$  similar to the Matthiessen rule in metals [35] but with an additional weight between the different processes. Here we present a relation of infinite matter collisional damping to  $\Gamma_{\text{coll}}$  and of the largest Lyapunov exponent of chaotic surface scattering to  $\Gamma_{\text{surf}}$  according to the ratio of the corresponding collision frequencies. Moreover the hypotheses by Swiatecki [36] that there is a chaotic mechanism of dissipation which over-damps octupole modes caused by negative curved surfaces is questioned. We will find that the octupole deformation does not lead to any special enhancement of the Lyapunov exponent in comparison with the quadrupole mode. Instead any deformation will cause a contribution to the damping of collective modes.

The outline of the paper is as follows. In the next chapter II we calculate the largest Lyapunov exponent for a nucleon in a deformed nucleus. Then in chapter III we derive a unified response function which combines both the collisional damping and the contribution from the surface scattering. In chapter IV we compare both damping contributions with the experimental values of hot isovector giant dipole resonances (IVGDR). A proper weighting corresponding to the relative collision frequencies yields us a unified picture which describes the data well and shows the relative importance of collisional contributions at small temperatures and of surface deformations at higher experimental excitations. Chapter V will

than summarize the results.

## II. LARGEST LYAPUNOV EXPONENT OF DEFORMED NUCLEI

We will consider in the following only classical 3-D closed billiards and can use the largest Lyapunov exponent as a relevant measure to characterize chaoticity. The surface of these billiards is chosen to resemble the surface deformation of a nucleus undergoing quadrupole or octupole deformations at fixed time.

The Lyapunov exponent can be given as the time derivative of the difference of the trajectories

$$|\vec{r}_1(t) - \vec{r}_2(t)| = |\vec{r}_1(0) - \vec{r}_2(0)| e^{\lambda t} \quad (1)$$

as

$$\lambda = \lim_{t \rightarrow \infty} \lim_{\varepsilon \rightarrow 0} \frac{1}{t} \ln \frac{|\vec{r}_1(t) - \vec{r}_2(t)|}{|\vec{r}_1(0) - \vec{r}_2(0)|}. \quad (2)$$

For  $\lambda > 0$  we have an exponential growing apart of the difference in phase space leading to chaotic behavior.

We solve the Hamilton equations for one particle in finite nuclear matter with an infinite potential\*

$$V(r, \theta) = V_0 \Theta(r - R(\theta)) \quad (3)$$

modeling the deformation of a radial symmetric nuclear surface

$$R_\lambda(\theta) = R_0 (1 + \alpha_{00} + \alpha_\lambda P_\lambda(\cos(\theta))) \quad (4)$$

with  $\lambda = 2$  corresponding to the quadrupole and  $\lambda = 3$  to the octupole deformations [37]. The  $\alpha_{00}$  is adjusted to conserve the volume for incompressible nuclear matter.

---

\*The numerical implementation is performed with  $[V_0 \rightarrow \infty]$  and  $\sigma \rightarrow 0$ ]

$$V(r, \theta) \approx V_0 \left( \arctan \left( \frac{r - R(\theta)}{\sigma} \right) + \frac{\pi}{2} \right)$$

resembling an infinite step function.

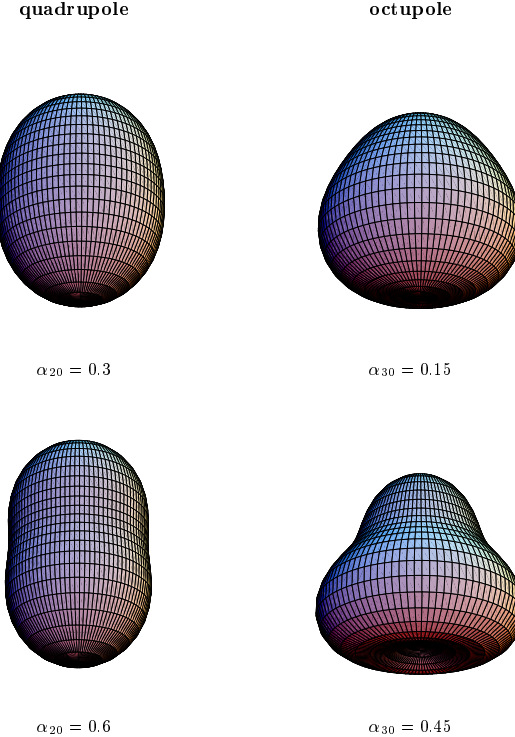


FIG. 1. Overview of the geometry of modes

The Lyapunov exponent is calculated by considering the time evolution of small deviations from a reference trajectory due to infinitesimal initial changes. We have used the Brandstaetter method resetting the deviations of the reference trajectory repeatedly after a certain time to the initial infinitesimal deviations. This way an averaging is performed and the largest mean Lyapunov exponent is obtained.

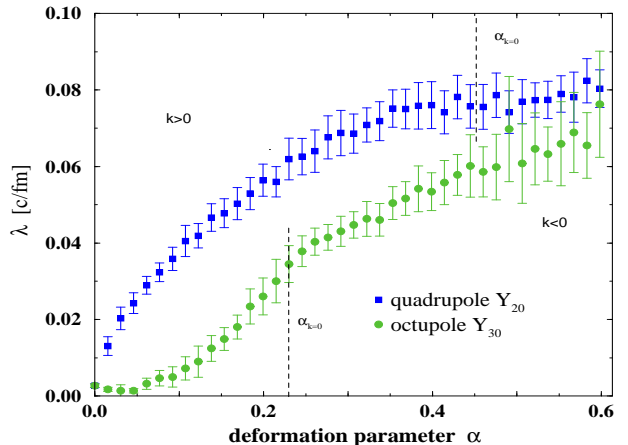


FIG. 2. The largest Lyapunov exponent of a spherical deformed billiard versus deformation parameter (4). The region of  $\alpha$  where the surface starts to become negative curved ( $k < 0$ ) for some special angle via (5) are indicated by dotted lines  $\alpha_{k=0}$  for octupole and quadrupole deformation separately.

In figure 2 we calculated the Lyapunov exponent for different octupole and quadrupole deformations according to (4). The error bars are taken from averaging 50 runs of different initial conditions indicating 95% confidence level. We see that the quadrupole deformation leads to an immediate increase of Lyapunov exponent while the Lyapunov exponent of the octupole increases later and more slowly with increasing deformation. Let us note here already that the characteristic time scales from the Lyapunov exponent are similar to the damping rate of IVGDR which will be presented in figure 4. This motivates us to consider a unified response from collisions and surface contributions.

As was pointed out in [36] a surface with negative curvature should induce a new chaotic mechanism analogous to Sinai billiard. We discuss therefore the curvature of a rotation body given by the curvature of the boundary curve  $R(\theta)$  of (4) via

$$k = \frac{R^2 + 2R'^2 - RR''}{(R^2 + R'^2)^{3/2}} \quad (5)$$

where  $R'$  and  $R''$  denote the derivatives with respect to  $\theta$ . In figure 2 we see that the octupole deformation shows parts with negative curvature earlier than the quadrupole. No significant difference occurs above this point. We can therefore conclude that the octupole deformation compared with the quadrupole deformation leads to no significantly different behavior and we see no specific chaotization in octupole deformations.

### III. DAMPING OF COLLECTIVE OSCILLATIONS

Since the largest Lyapunov exponent in slightly deformed nuclei has led to time scales comparable with the damping rate of IVGDR, we would like now to focus on a unified description of the linear response including collisional contributions and chaotic scattering with the surfaces. Therefore let us first briefly sketch the response function formalism starting from appropriate kinetic equations. For infinite matter this will result in the known Mermin response function which has been used to describe the IVGDR in symmetric [10] and asymmetric nuclear matter [12]. Then we will proceed and derive the response function for finite nuclei and show that in a local density approximation chaotic scattering from the surface can be incorporated. The result will be a Mermin like response function in local density approximation where the largest Lyapunov exponent appears as an imaginary shift in the frequency.

#### A. Infinite matter response

The concept of collisional damping starts from an interacting many body system where the quasiclassical particles with position  $r_i$  and momenta  $p_i$  fulfill the Hamil-

tonian equations. The corresponding quasiclassical distribution function for protons or neutrons  $f(p, r, t)$

$$f(p, r, t) = \frac{1}{V} \sum_i \delta(r - r_i(t)) \delta(p - p_i(t)) \quad (6)$$

satisfy the Vlasov equation  $[I(p, r, t) = 0]$

$$\dot{f}(p, r, t) + \frac{p}{m} \partial_r f(p, r, t) - \partial_r V \partial_p f(p, r, t) = I(p, r, t) \quad (7)$$

with the self-consistent mean-field potential for the neutrons  $V$  in a schematic Skyrme type [38,39]

$$\begin{aligned} V(r, t) = t_0 & \left\{ \left(1 + \frac{x_0}{2}\right) (n_n(r, t) + n_p(r, t)) \right. \\ & - \left. \left(x_0 + \frac{1}{2}\right) n_n(r, t) \right\} \\ & + \frac{t_3}{4} \left\{ (n_n(r, t) + n_p(r, t))^2 - n_n^2(r, t) \right\} \end{aligned} \quad (8)$$

where the neutron and proton densities are  $n_n$  and  $n_p$  and the parameters are  $x_0 = 0.48$ ,  $t_0 = -983.4$  MeV fm<sup>3</sup> and  $t_3 = 13106$  MeV fm<sup>6</sup>. The corresponding proton mean field is given by interchanging the densities. In order to consider collisions on the right-hand side of (7) one should include an appropriate collision integral.

#### 1. Collision free

The collective effects can be obtained from the linearization of the Vlasov equation with respect to an external potential  $\delta V_{\text{ext}}$ . The induced density is then obtained by (7) in the form

$$\delta n = \Pi_0(\delta V_{\text{ext}} + \frac{\partial V}{\partial n} \delta n). \quad (9)$$

The complete polarization function  $\Pi$  connects the induced density fluctuation  $\delta n$  with the external potential via

$$\delta n = \Pi \delta V_{\text{ext}} \quad (10)$$

and for homogeneous systems the polarization function can be read off from (9) for infinite matter

$$\Pi^{\text{inf}}(q, \omega) = \frac{\Pi_0^{\text{inf}}(q, \omega)}{1 - V_0 \Pi_0^{\text{inf}}(q, \omega)} \equiv \frac{\Pi_0^{\text{inf}}(q, \omega)}{\epsilon(q, \omega)} \quad (11)$$

with the Lindhard function

$$\Pi_0^{\text{inf}}(q, \omega) = 4 \int \frac{dp'}{(2\pi\hbar)^3} \frac{q \partial_{p'} f_0(p')}{\frac{p' q}{m} - \omega} \quad (12)$$

and  $V_0 = \frac{\partial V}{\partial n}$ . For isovector oscillations where the density variation  $\delta n$  is considered to be the difference between proton and neutron densities we have from (8)

$$V_0 = -\frac{t_0}{2} \left( x_0 + \frac{1}{2} \right) - \frac{t_3}{8} n_0 \quad (13)$$

where  $n_0 = 0.16 \text{ fm}^{-3}$  is the nuclear saturation density.

Now the zeros  $\omega = \Omega + i\gamma$  of the dielectric function  $\epsilon(q, \omega) = 0$  in (11) determine now the collective modes with the energy  $\Omega$  and the Landau damping  $\gamma$  of the collective excitation. Within a schematic model [40] the wave vector scales like  $q = \frac{\pi}{2R_0}$  with the nuclear radius  $R_0 = r_0 A^{1/3}$  and  $r_0 = 1.13 \text{ fm}$ .

## 2. Collisional damping model

In order to take collisions into account as a further damping effect beyond Landau damping, we start from a kinetic equation analogous to (7) but with an additional collisional term  $I[p, r, t]$  on the right hand side. In [10] we have derived a collision integral in a non-Markovian relaxation time approximation

$$I(p, r, t) = \int_0^t \frac{\tilde{f}(p, r, \bar{t}) - f(p, r, \bar{t})}{\tau(t - \bar{t})} d\bar{t} \quad (14)$$

with the dynamical non-Markovian relaxation time

$$\frac{1}{\tau_m(\omega)} = \frac{1}{\tau_B} \left[ 1 + \frac{3}{4} \left( \frac{\omega}{\pi T} \right)^2 \right]. \quad (15)$$

The Markovian relaxation time is given by  $\tau_B^{-1} = \frac{8\pi m}{3\hbar^3} \sigma T^2$ , where  $\sigma$  is the averaged spin-isospin proton-neutron cross section. This collision integral holds for low temperatures compared to the Fermi energy in the sense of the Sommerfeld expansion. The non-Markovian relaxation time arises from the coupling of collective modes regarding two particle scattering and describes consequently the effect of zero sound damping. The local equilibrium distribution  $\tilde{f}$  is determined through the conservation of the local current. The linearization of the kinetic equation leads then to the extended response function of Mermin [41] to incorporate the collision effects into the response function

$$\Pi_0^M(q, \omega) = \frac{\Pi_0^{\text{inf}}(q, \omega + \frac{i}{\tau})}{1 - \frac{i}{\omega\tau + i} \left( 1 - \frac{\Pi_0^{\text{inf}}(q, \omega + \frac{i}{\tau})}{\Pi_0^{\text{inf}}(q, 0)} \right)}, \quad (16)$$

where the selfconsistency leads to the replacement of  $\Pi_0^{\text{inf}}$  by  $\Pi_0^M$  in (11).

The energy and damping rates are now determined by the zeros of the (Mermin) response function [10]

$$\epsilon^M(q, \Omega + i\gamma) = 1 - V_0(q) \Pi_0^M(q, \Omega + i\gamma) = 0. \quad (17)$$

Here the damping rate represent Landau and collisional damping.

## B. Finite matter response

In the next step we will present the finite matter response function in terms of a memory integral over all trajectories. This allows us to introduce the local density approximation as a first order memory effect in the trajectories. To this end we rewrite the Vlasov equation (7) in a slightly different way. Introducing the Lagrange picture by following the trajectory  $x(t), p(t)$  of a particle we linearize the Vlasov equation (7) according to  $f(x, p, t) = f_0(x, p) + \delta f(x, p, t)$  as

$$\frac{d}{dt} \delta f(x(t), p(t), t) = \partial_p f_0 \partial_{x(t)} \delta V \quad (18)$$

and get with one integration

$$\delta f(x, p, t) = -2m \int_{-\infty}^0 dt' \int_{-\infty}^{\infty} dx' \frac{d}{dt'} \delta(x' - x(t')) \frac{\partial f_0(p^2, x')}{\partial p^2} \delta V(x', t + t'). \quad (19)$$

The density variation caused by varying the external potential is then obtained as

$$\delta n(x, \omega) = -2ms \int dx' \int \frac{dp^3}{(2\pi\hbar)^3} \partial_{p^2} f_0(p^2, x') \times \int_{-\infty}^0 dt' e^{-it'\omega} \frac{d}{dt'} \delta(x' - x(t')) \delta V(x', \omega) \quad (20)$$

where  $s$  denotes the spin-isospin degeneracy. Comparing this expression with the definition of the polarization function  $\Pi_0$ ,

$$\delta n(x, \omega) = \int dx' \Pi_0(x, x', \omega) \delta V(x', \omega), \quad (21)$$

we are able to identify the polarization of finite systems as

$$\Pi_0(x, x', \omega) = -2ms \int \frac{dp^3}{(2\pi\hbar)^3} \partial_{p^2} f_0(p^2, x') \times \int_{-\infty}^0 dt' e^{-it'\omega} \frac{d}{dt'} \delta(x' - x(t')). \quad (22)$$

Further simplifications are possible if we focus on the ground state  $f_0(p^2) = \Theta(p_f^2 - p^2)$ . The modulus integration of momentum can be carried out and the Kirschnitz-formula [42,43] appears

$$\Pi_0(x, x', \omega) = -\frac{ms p_f(x)}{4\pi^2\hbar^3} \left[ \int_{-\infty}^0 dt' e^{-it'\omega} \frac{d}{dt'} \int \frac{d\Omega_p}{4\pi} \delta(x' - x(t')) \right]$$

$$= -\frac{msp_f(x)}{4\pi^2\hbar^3} \left[ \delta(x' - x(0)) + i\omega \int_{-\infty}^0 dt' e^{-it'\omega} \int \frac{d\Omega_p}{4\pi} \delta(x' - x(t')) \right]. \quad (23)$$

This formula represents the ideal free part and a contribution which arises by the trajectories  $x(t)$  averaged over the direction at the present time  $\vec{n}_p p_f = m\dot{\vec{x}}(0)$ . In principle, the knowledge of the evolution of all trajectories is necessary to evaluate this formula. Molecular-dynamical simulations can perform this task but it requires an astronomical amount of memory to store all trajectories. Rather, we discuss two approximations which will give us more insight into the physical processes behind. First the radical one shows how the local density approximation emerges. In the next one we consider the influence of chaotic scattering on a surface.

### 1. Local density approximation

The local density approximation appears from (23) when we perform two simplifications. Introducing Wigner coordinates  $R = (x + x')/2$ ,  $r = x - x'$  we have to assume

1. gradient expansion

$$p_f(R + \frac{r}{2}) \approx p_f(R) + \mathcal{O}(\partial_R) \quad (24)$$

2. expansion of the trajectories to first order history

$$x' - x(t') \approx -r - t'\dot{x} = -r - t'\frac{p_f}{m}\vec{n}_p + \mathcal{O}(t'^2). \quad (25)$$

With these two assumptions we obtain from (23) after trivial integrations

$$\Pi_0^{\text{LDA}}(q, R, \omega) = -\frac{msp_f(R)}{4\pi^2\hbar^3} \left\{ 1 + ik \int_0^\infty dy e^{iky} \frac{\sin y}{y} \right\} \quad (26)$$

where  $k = m\omega/q/p_f(R)$ . This can be further integrated with the help of

$$\begin{aligned} \int_0^\infty dy e^{iky} \frac{\sin y}{y} &= \arctan(\text{Im } k - i\text{Re } k)^{-1} \\ &= 2i \ln \left( \frac{1+k}{1-k} \right) + \pi [\text{sgn}(1+k) + \text{sgn}(1-k)] \Big|_{\text{Im } k \rightarrow 0} \end{aligned} \quad (27)$$

to yield the standard Lindhard result. We recognize the ground state result for infinite matter (12) except that

the Fermi momentum  $p_f(R)$  has to be understood as a local quantity corresponding to local densities so that we get

$$\Pi_0^{\text{LDA}}(q, R, \omega) = \Pi_0^{\text{inf}}(q, p_f(R), \omega). \quad (28)$$

For extensions beyond the local density approximation see [43,44].

### C. Influence of chaotic scattering with surface on damping

Now we focus on the influence of an additional chaotic scattering which will be caused e.g. by the curved surface. In order to investigate this effect we add to the regular motion (25) a small irregular part  $\Delta x$

$$x' - x(t') \approx -r - t'\frac{p_f}{m}\vec{n}_p + \Delta x. \quad (29)$$

The irregular part of the motion we specify in the direction of the current movement lasting a time  $\Delta_t$  and given by an exponential increase in phase-space controlled by the Lyapunov exponent  $\lambda$ . Therefore we can assume  $[t' < 0]$

$$\Delta_x \approx \frac{p_f \vec{n}_p}{m} \Delta_t \exp[-\lambda(t' - \Delta_t)] + \text{const.} \quad (30)$$

Since we are looking for the upper bound of Lyapunov exponent we can take (30) at the maximum  $\Delta_t = -1/\lambda$ . Further, we require, that in the case of vanishing Lyapunov exponent we should regain the regular motion (25). We obtain finally for (30)

$$x' - x(t') \approx -r - \frac{p_f}{m} \vec{n}_p \left[ \frac{1 - \exp(-\lambda t')}{\lambda} \right]. \quad (31)$$

With this ansatz one derives from (23) the result

$$\begin{aligned} \Pi(q, R, \omega) &= -\frac{msp_f(R)}{4\pi^2\hbar^3} \left[ \right. \\ &\quad \left. 1 + ik \int_0^\infty dy \frac{\sin y}{y} \left( 1 + \frac{ky}{\omega} \lambda \right)^{i\omega/\lambda-1} \right], \end{aligned} \quad (32)$$

instead of (26) which for  $\lambda \rightarrow 0$  resembles exactly (26). The further integration could be given in terms of hypergeometric functions but this is omitted here.

With this formula we have derived the main result of this section which leads to a polarization function due to many particle effects including the influence of an additional chaotic process characterized by the Lyapunov exponent  $\lambda$ .

For small values of  $(m/q p_f)\lambda = k\lambda/\omega$  which corresponds to relatively small Lyapunov exponents, we can use

$\lim_{x \rightarrow \infty} (1 + a/x)^x = \exp(a)$  in the integral of (32) and the final integration is performed gaining the result of (28) but with a complex shift

$$\Pi_0^{\text{surf}}(q, R, \omega) = \Pi_0^{\text{inf}}(q, p_f(R), \omega + i\lambda). \quad (33)$$

Solving now the dispersion relation we would obtain by this way just the known Matthiessen rule which states that the damping mechanisms are additive in the damping. However we have to consider that the collisional damping of infinite matter  $2\gamma$  and the largest Lyapunov exponent  $\lambda$  for a single particle calculated in chapter II are related to these two damping mechanisms  $\Gamma_{\text{coll}}$  and  $\Gamma_{\text{surf}}$  by a proper relative weight. This weight will be given just by the relative occurrence of the processes, the collisions with other particles and the collisions with surface.

#### IV. COMPARISON OF DAMPING MECHANISMS

##### A. Connection between surface curvature and temperature

The damping of excited nuclei is controlled by two different mechanisms. Besides the collisional damping we also have to consider the shape fluctuation. In the absence of inertia, assumed in the following, the driving force for shape fluctuations is the temperature. Therefore we link the surface deformation  $\alpha$  of (4) to the temperature within a statistical model. We use as mean deformation

$$\langle \alpha \rangle = \frac{\int d\alpha \alpha \exp(-E_B(\alpha)/T)}{\int d\alpha \exp(-E_B(\alpha)/T)} \quad (34)$$

where the surface dependent energy  $E_B(\alpha)$  is given by the Bethe-Weizsäcker formula <sup>†</sup>

$$E_B(\alpha) = -a_1 + \frac{a_2}{A^{1/3}} + \frac{a_3 Z^2}{A^{4/3}} + a_4 \delta^2 + a_5 A^{2/3} \frac{S(\alpha)}{S(0)} \quad (37)$$

---

<sup>†</sup>Please remind that in principle the Coulomb energy changes with small deformation as well according to the factor [45]

$$1 - 5 \frac{(\lambda - 1)}{(2\lambda + 1)^2} \alpha_\lambda^2 \quad (35)$$

while the surface term changes as

$$1 + (\lambda - 1)(\lambda + 2)/2/(2\lambda + 1) \alpha_\lambda^2. \quad (36)$$

While the latter correction is considered here the former would lead only to correction of around 0.3% and are neglected.

with the volume energy  $a_1 = 15.68$  MeV, Coulomb energy  $a_3 = 0.717$  MeV, the symmetry energy  $a_4 = 28.1$  MeV and the surface energy  $a_5 = 18.56$  MeV.

The surface of rotational deformed nuclei (4) is given by

$$S = 2\pi \int_{-1}^1 dx R \sqrt{R^2 + (1 - x^2) R'(x)^2} \quad (38)$$

from which we obtain for the quadrupole  $S_2$  and octupole  $S_3$  deformation (36)

$$\begin{aligned} \frac{S_2(\alpha)}{S(0)} &= 1 + \frac{2}{5} \alpha^2 + \mathcal{O}(\alpha^3) \\ \frac{S_3(\alpha)}{S(0)} &= 1 + \frac{5}{7} \alpha^2 + \mathcal{O}(\alpha^3). \end{aligned} \quad (39)$$

This represents the lowest order expansion in  $\alpha$ , however the next term gives only corrections in fractions of percents for the highest deformations considered here. The statistical model (34) leads therefore to a connection between temperature and deformation as

$$T = c\pi a_5 A^{2/3} < \alpha >^2 \quad (40)$$

where the constant  $c$  is given by the coefficient of  $\langle \alpha \rangle^2$  in Eq. (39) for the corresponding deformations.

##### B. Finite matter scaling for collisional damping

According to the local density approximation (28) or (33) we now want to investigate the collisional damping in finite matter. Therefore we have to replace all densities in the dispersion relation (16) by the local density which are parameterized by a Woods-Saxon potential

$$n(r) = \frac{n_0}{\exp[(r - R_0)/0.545 \text{ fm}] + 1}. \quad (41)$$

Solving the dispersion relation (17) within the local density approximation according to (28) we obtain a spatial dependent damping rate  $\gamma(r)$ .

In the following we consider a finite size scaling  $\xi_A$  of the damping which approximates the local ( $r$ -dependent) dispersion relation by an averaged one

$$\langle \dots \rangle = \frac{3}{R_0^3} \int_0^{R_0} r^2 \dots dr \quad (42)$$

assuming radial symmetry. The finite size scaling

$$\xi_A = \frac{\langle \gamma(r) \rangle}{\gamma}, \quad (43)$$

which has to be applied to the infinite matter bulk collisional damping is  $\xi_{\text{Sn}} = 0.9199$  and  $\xi_{\text{Pb}} = 0.9250$  for  $^{120}\text{Sn}$  and  $^{208}\text{Pb}$  respectively. The bulk matter value of damping is therefore diminished by finite size effects.

### C. Comparison of collisional damping and surface damping

Using Eq. (40) we can now relate the Lyapunov exponent  $\lambda$  calculated in figure 2 as a function of deformation to the temperature. In figure 3 the contribution to the damping of IVGDR for  $^{120}\text{Sn}$  (circles) and  $^{208}\text{Pb}$  (squares) is presented for different shape deformations versus temperature. If we add quadrupole and octupole deformations we come up with a damping curve very similar to the paper of Ormand [21]. The damping starts at zero and increases rapidly with increasing temperature. We now see that the main contribution comes from the quadrupole deformation while the octupole deformation is sizeable at higher temperature only. Let us note that the qualitative difference between Sn and Pb is reproduced by surface scattering as well as collisional damping.

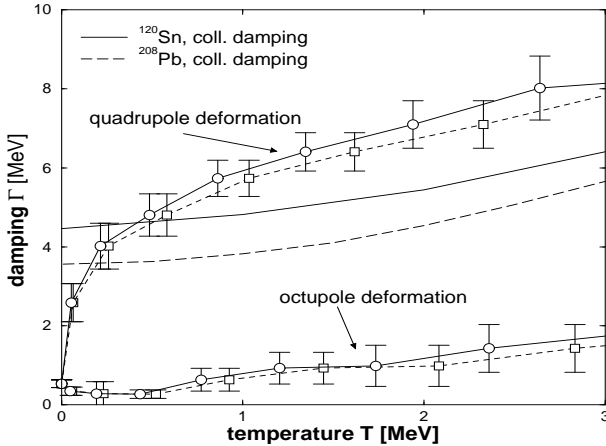


FIG. 3. The collisional damping scaled with finite size according to (43) is compared with the damping according to the chaotic scattering from the surface of quadrupole and octupole deformed shapes for  $^{120}\text{Sn}$  and  $^{208}\text{Pb}$  from figure 2.

The collisional contribution  $2\gamma$  scaled to finite sizes via (43) are plotted as well (Sn: solid line, Pb: dashed line). We recognize that both contributions by itself, collisional as well as surface scattering, account almost for the same amount required for the experimental values in figure 4. A proper relative weight of both processes should be considered which will be introduced in the following.

So far we have not considered that in the presence of collisions only particles close to the surface can appreciably contribute to the surface chaotization, while particles deep inside the nuclei are screened out of this process. We consider therefore a single particle scattering from other particles at the collision frequency or inverse relaxation time  $1/\tau_M$ . This has to be compared with the collision frequency of the particle hitting the surface increase beyond the sphere since for a sphere we do not have a Lyapunov exponent. This additional surface collision frequency  $\nu_{\text{surf}}$  is given by the product of density with the surface  $S(\alpha) - S(0) = c\alpha^2 4\pi R_0^2$  according to Eq.

(39) and the mean velocity in radial direction  $v_r = 3/8v_F$  resulting into

$$\nu_{\text{surf}} = 1.5Tn_0v_Fr_0^2/a_5 \quad (44)$$

where we have used Eq. (40) to replace  $\alpha$ . We see that this frequency is independent of the nucleus and linearly dependent on temperature.

It is now evident that the ratio of the collisional and surface-hitting frequencies gives the proper weight of both collisional and surface damping processes. Consequently the width including the correct weighting factor of the damping processes reads

$$\begin{aligned} \Gamma_{\text{FWHM}} &= \zeta 2 < \gamma(r) > + (1 - \zeta) 2\lambda \\ &\equiv \Gamma_{\text{coll}} + \Gamma_{\text{surf}}. \end{aligned} \quad (45)$$

With the help of (15) and (44) the weighting factor is given by

$$\zeta(T) = \frac{\frac{1}{\tau_M}(T)}{\frac{1}{\tau_M}(T) + \nu_{\text{surf}}(T)}. \quad (46)$$

One sees that for zero and high temperatures  $\zeta = 1$  and due to Eq. (45) only the collisional contributions matters. Since  $\nu_{\text{surf}}$  goes proportional to and  $1/\tau$  depends quadratically on temperature, the weighting factor  $\zeta$  has a minimum at temperatures around  $T = \frac{\sqrt{3}}{2\pi}\omega$  and the surface contributions become important. In the case of IVGDR this corresponds to a temperature of  $T \approx 3.7\text{ MeV}$ , which is the upper limit of current experimental achievable temperatures. Therefore we can state that at low temperatures the collisional damping is dominant and at higher temperatures the surface contribution becomes significant.

In figure 4 we compare the effective damping according to Eq. (45) with the experimental data. We find reasonable quantitative agreement.

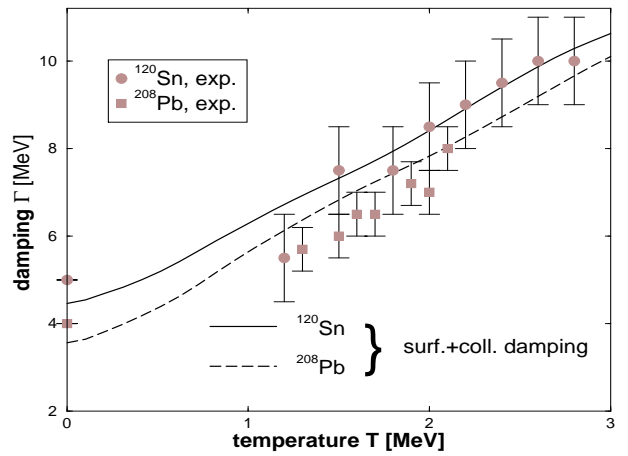


FIG. 4. The effective damping consisting of collisional and surface damping together with the experimental data (filled symbols) from Ref. [46] (Sn) and from Ref. [47] (Pb).

While the collisional damping by itself can reproduce the increase at small temperatures well enough it fails to reproduce the sharp rise at higher temperatures. The surface damping by itself fails at zero temperature and leads to an unphysical shape. Only the connection of both effects, collisional and surface damping can reproduce the data correctly.

## V. SUMMARY

We have considered the influence of collisional damping as well as surface scattering for the damping of isovector giant dipole resonances (IVGDR). We find that the relative importance of both effects is dependent on the temperature scale. While for low and high temperatures the collisional contribution dominates, the surface scattering is the one of significant importance at temperatures around one third of the centroid energy.

The surface contribution has been calculated from the Lyapunov exponent of surface scattering for different deviations of the nucleus shape. The deviations are related to the temperature by a statistical model which in turn allows one to compare the temperature dependence of collisional and surface damping.

The influence of both the surface and collisional damping is described by a generalized response function for finite nuclear matter which takes into account the chaotic processes of scattering with the surface. We derive this way a response function similar to the Lindhard response in local density approximation which is now modified by the Lyapunov exponent of the additional scattering process. In an approximative way we show that the total damping is described by the sum of two contributions to the damping in analogy to the Matthiessen rule.

Comparing the proper collision frequency for one particle with other particles and with the surface respectively we derive a proper relative weight for both processes, the collisional and surface damping. The resulting effective damping reproduces the experimental data rather well in the whole accessible range.

## ACKNOWLEDGMENTS

The authors are especially indebted to A. Dellafiore for bringing the Kirshnitz formula to our attention. M. DiToro is thanked for many discussions and Hans J. Weber for helpfull comments. The work was supported by the BMBF (Germany) under contract Nr. 06R0884, the DFG under contract Nr. 905-13/1 and the Max-Planck Society.

- [1] S. Kamerdzhev, *Yad. Fiz.* **9**, 324 (1969).
- [2] H. Sagawa and G. F. Bertsch, *Phys. Lett. B* **5**, 138 (1984).
- [3] V. Abrosimov, M. Di Toro, and A. Smerzi, *Z. Phys. A* **347**, 161 (1994).
- [4] V. Kolomietz, V. Pluiko, and S. Shlomo, *Phys. Rev. C* **52**, 2480 (1995).
- [5] V. Kolomietz, V. Plujko, and S. Shlomo, *Phys. Rev. C* **54**, 3014 (1996).
- [6] V. Kondratyev and M. Di Toro, *Phys. Rev. C* **53**, 2176 (1996).
- [7] E. Hernández, J. Navarro, A. Polls, and J. Ventura, *Nucl. Phys. A* **597**, 1 (1996).
- [8] M. Di Toro, V. Kolomietz, and A. Larionov, in *Proceedings of the Dubna Conference on Heavy Ions*, Dubna, 1997 (unpublished).
- [9] V. Kolomietz, A. Larionov, and M. Di Toro, *Nucl. Phys. A* **613**, 1 (1997).
- [10] U. Fuhrmann, K. Morawetz, and R. Walke, *Phys. Rev. C* **58**, 1473 (1998).
- [11] V. M. Kolomietz, S. V. Lukyanov, V. A. Plujko, and S. Shlomo, *Phys. Rev. C* **58**, 198 (1998).
- [12] K. Morawetz, R. Walke, and U. Fuhrmann, *Phys. Rev. C* **57**, 2813 (1998).
- [13] S. Ayik, O. Yilmaz, A. Golkalp, and P. Schuck, *Phys. Rev. C* (in press).
- [14] G. Gervais, M. Thoennessen, and W. E. Ormand, *Phys. Rev. C* (in press).
- [15] S. Shlomo and G. F. Bertsch, *Nucl. Phys. A* **243**, 507 (1975).
- [16] H. Esbensen and G. F. Bertsch, *Phys. Rev. C* **28**, 355 (1983).
- [17] H. Esbensen and G. F. Bertsch, *Ann. Phys.* **157**, 255 (1984).
- [18] P. F. Bortignon, A. Bracco, D. Brink, and R. A. Broglia, *Phys. Rev. Lett.* **67**, 3360 (1991).
- [19] W. E. Ormand, P. F. Bortignon, and R. A. Broglia, *Phys. Rev. Lett.* **77**, 607 (1996).
- [20] S. Kamerdzhev, J. Speth, and G. Tertychny, *Nucl. Phys. A* **624**, 328 (1997).
- [21] W. E. Ormand, P. F. Bortignon, R. A. Broglia, and A. Bracco, *Nucl. Phys. A* **614**, 217 (1997).
- [22] S. Kamerdzhev, R. J. Liotta, E. Litvinova, and V. Tselyaev, *Phys. Rev. C* **58**, 172 (1998).
- [23] J. Kvasil, N. L. Iudice, V. O. Nesterenko, and M. Kopal, *Phys. Rev. C* **58**, 209 (1998).
- [24] Y. Alhassid and B. Bush, *Phys. Rev. Lett.* **63**, 2452 (1989).
- [25] W. E. Ormand *et al.*, *Phys. Rev. Lett.* **64**, 2254 (1990).
- [26] W. E. Ormand *et al.*, *Phys. Rev. Lett.* **69**, 2905 (1992).
- [27] B. Lauritzen, P. F. Bortignon, R. A. Broglia, and V. G. Zelevinsky, *Phys. Rev. Lett.* **74**, 5190 (1995).
- [28] A. Bracco *et al.*, *Phys. Rev. Lett.* **74**, 3748 (1995).
- [29] S. Leoni, T. Dössing, and B. Herskind, *Phys. Rev. Lett.* **76**, 4484 (1996).
- [30] M. Colonna *et al.*, *Phys. Lett. B* **307**, 293 (1993).
- [31] V. Baran *et al.*, *Nucl. Phys. A* **599**, 29 (1996).
- [32] K. Morawetz and R. Walke, *Phys. Rev. C* (1998), sub.
- [33] V. Špička, P. Lipavský, and K. Morawetz, *Phys. Lett. A* **240**, 160 (1998).
- [34] D. Brink, A. Dellafiore, and M. DiToro, *Nucl. Phys. A*

**456**, 205 (1986).

- [35] N. F. Mott and H. Jones, *The Theory of the Properties of Metals and Alloys* (Oxford University Press, London, 1936).
- [36] J. Blocki, J.-J. Shi, and W. Swiatecki, Nucl.Phys **A554**, 387 (1993).
- [37] P. Ring and P. Schuck, *The Nuclear Many-Body Problem* (Springer-Verlag, New York, 1980).
- [38] D. Vautherin and D. Brink, Phys. Rev. C **5**, 626 (1972).
- [39] F. Braghin and D. Vautherin, Phys. Lett. B **333**, 289 (1994).
- [40] H. Steinwedel and J. Jensen, Z. Naturforsch. **5**, 413 (1950).
- [41] N. Mermin, Phys. Rev. B **1**, 2362 (1970).
- [42] D. Kirzhnitz, Y. Lozovik, and G. Shpatakovskaya, Usp. Fiz. Nauk **117**, 3 (1975).
- [43] A. Dellafiore, F. Matera, and D. M. Brink, Phys. Rev. A **51**, 914 (1995).
- [44] A. Dellafiore and F. Matera, Phys. Rev. A **41**, 4958 (1990).
- [45] W. Greiner and J. Maruhn, *Nuclear Models* (Springer-Verlag, Berlin et.al, 1996).
- [46] E. Ramakrishnan *et al.*, Phys. Rev. Lett. **76**, 2025 (1996).
- [47] E. Ramakrishnan *et al.*, Nucl. Phys. **A549**, 49 (1996).